Pis'ma v ZhETF, vol. 93, iss. 10, pp. 674 – 683

ПО ИТОГАМ ПРОЕКТОВ
РОССИЙСКОГО ФОНДА ФУНДАМЕНТАЛЬНЫХ ИССЛЕДОВАНИЙ
Проект РФФИ # 08-02-00098а

Recent experimental results on the superconductor/ferromagnet proximity effect

I. A. Garifullin[1)]

Zavoisky Physical-Technical Institute, Kazan Scientific Center RAS, 420029 Kazan, Russia

Submitted 31 March 2011

The recent experimental results on the proximity effect in heterostructures composed of superconducting and ferromagnetic thin films are reviewed. First, the experimental observation and investigation of the spin screening effect, i.e., a spin polarization in the V layer developing in the superconducting state under the influence of a spin polarization of conduction electrons in the ferromagnetic layer are discussed. This effect was predicted theoretically by Bergeret et al. [F.S. Bergeret, A.F. Volkov, and K.B. Efetov, EPL **66**, 111 (2004); Phys. Rev. B **69**, 174504 (2004)]. Then, the progress concerning the experimental realization of the superconducting spin switch device based on the superconductor/ferromagnet proximity effect is presented.

1. Introduction. The mutual influence of magnetism and superconductivity in superconductor/ferromagnet (S/F) nanofabricated thin film heterostructures has been an exciting topic in Solid State Physics during the last 15 years (see, e.g., the reviews [1–5]). As emphasized frequently in these reviews, the antagonism of superconductivity (S) and ferromagnetism (F) consists of strong suppression of superconductivity by ferromagnetism because ferromagnetism requires parallel (P) and superconductivity requires antiparallel (AP) orientation of spins. The exchange splitting of the conduction band in strong ferromagnets which tends to align electron spins parallel is larger by orders of magnitude than the coupling energy for the AP alignment of the electron spins in the Cooper pairs in conventional superconductors. Therefore the singlet pairs with AP spins of electrons will be strongly destroyed by the exchange field. For this reason the Cooper pairs can penetrate into an F layer only over a small distance ξ_F. In this case the Cooper pair wave function which penetrates from a superconductor into a ferromagnet exhibits a damped oscillating behavior because of the non-zero momentum of the Cooper pairs in the F layer. The characteristic depth of the decay of the pairing function in the F layer $\xi_F = (4\hbar D_F/I)^{1/2}$ is determined by the the diffusion coefficient D_F and the exchange splitting I of the conduction band in the F layer [6]. For pure Fe the value of ξ_F is less than 1 nm (see, e.g., [7]).

One might ask intuitively, whether the reverse effect, namely an S layer attaining a spontaneous magnetic moment at the S/F interface, is also possible. Actually this really should happen as has been proven theoretically [8, 9]. Originally in Ref. [8] this phenomenon was called the inverse proximity effect. Qualitatively the physical origin of this effect can easily be understood. Let us consider an S/F bilayer with the F layer being thin compared to ξ_F. Due to the exchange field the conduction electron spins in the F layer are polarized in one direction predominantly. These electrons have their Cooper partners deep in the S layer on the distance ξ_s which is the superconducting (SC) coherence length. Thus, due to the SC correlations, a spin polarization is induced in the S layer. The magnetic moment in the S layer should be oriented antiparallel to the magnetization of conduction electrons in the F layer. Theoretically, for a very thin F layer the induced magnetic moment of conduction electrons in the S layer should exactly compensate the moment of conduction electrons in the F layer [9]. This is the reason why we use the term *spin screening effect* instead of *inverse proximity effect*, because it characterizes the physical situation more precisely.

There is another interesting theoretical prediction still waiting for an experimental realization. This is the spin valve effect based on the S/F proximity effect. The physical origin of this effect relies on the idea to control the pair-breaking, and hence the SC transition temper-

1)e-mail: ilgiz_garifullin@yahoo.com

ature T_c, by manipulating the mutual orientation of the magnetizations of the F layers in a heterostructure comprising, e.g., two F and one S layer in a certain combination. This is because the mean exchange field from two F layers acting on Cooper pairs in the S layer is smaller for the AP orientation of the magnetizations of these F layers compared to the P case.

Historically, the first paper devoted to the realization of the spin switch effect by manipulating the mutual orientation of the magnetization of the F layers has been published by Deutscher and Meunier in 1969 [10]. They studied FeNi/In/Ni trilayer and obtained a surprisingly large difference in T_c between the AP and P orientations of the magnetizations $\Delta T_c = T_c^{AP} - T_c^{P}$. The reason for this big effect has not been clarified up to now. Clinton and Johnson [11] have developed a SC valve which uses the magnetic fringe fields at the edges of the F film of a μm size. Due to the stripe shape of the F film these fringe fields can be varied in magnitude by changing the orientation of the magnetization of the F layer. In this experiment a direct contact between F and S layers was absent similar to the case studied in Ref. [10]. The latter means that the experiments of Deutscher and Meunier have nothing common with S/F proximity effect. The possibility to develop a real switch based on the S/F proximity effect has been theoretically substantiated in 1997 by Oh et al. [12]. They proposed the F1/F2/S layer scheme where an S film is deposited on top of two F layers. The thickness of F2 should be smaller than ξ_F to allow the SC pair wave function to penetrate into the space between F1 and F2 layers. Two years later a different construction based on an F/S/F trilayer was proposed theoretically by Tagirov [13] and Buzdin et al. [14]. Several experimental works confirmed the predicted influence of the mutual orientation of the magnetizations in the F/S/F structure on T_c (see, e.g., [15–18]). However, the difference in T_c between the AP and P orientations ΔT_c turns out to be smaller than the width of the SC transition δT_c itself. Hence a full switching between the normal and the SC state was not achieved. Implementation of a design similar to the F1/N/F2/S layer scheme by Oh et al. [12] with a $[\mathrm{Fe/V}]_n$ antiferromagnetically coupled superlattice instead of a single F1/N/F2 trilayer [19] is not actually the spin switch device because the system can not be switched from the AP to P orientations of the magnetizations instantaneously. At the same time the analysis of the temperature dependence of the critical field has shown that implicitly ΔT_c of this system can reach up to 120 mK at $\delta T_c \sim 100$ mK.

The paper is organized as follows. First, the results of the first observation and investigation of the spin screening effect in the S/F layered structures are analyzed. Then, the recent achievements in the realization of the spin valve effect are presented.

2. Spin screening effect. 2.1. *Necessary conditions for the observation of the spin screening effect.* For a real S/F bilayer the amplitude of the magnetization induced by the spin screening effect in the S layer is expected to be very small, and for an experimental proof of the spin screening effect one needs a method which can sensitively probe small changes of the spin polarization in the S layer below T_c. Principally one can investigate the penetration profile of the polarization of conduction electrons induced by the F layer within the S layer in the S/F bilayers using the technique of low-energy muon spin rotation. However, estimates show that detection of the effect is on the verge of sensitivity of this technique. The induced spin polarization in the SC state corresponds to a change of the spin susceptibility of the conduction electrons upon the SC transition. This spin susceptibility is one of the physical reasons for the Knight shift of the nuclear magnetic resonance (NMR) line in metals. Thus, in NMR the spin screening effect should manifest itself as a decrease of the Knight shift upon the transition to the SC state.

For our investigation [20, 21] of the spin screening effect by NMR the choice of an appropriate F/S material combination is of primary importance. It is desirable that the S-layer material has a strong NMR signal with a small linewidth, a suitable SC transition temperature T_c and a high quality interface with the F material. In addition, there should be an appreciable change of the Knight shift at the transition to the SC state. Among the elemental superconductors Pb, Nb and V appear to be possible candidates [22, 23]. However, only V fulfills the condition of a high interface quality with epitaxial growth of Fe on V and high interface transparency for the electrons [24, 25]. The early results of Noer and Knight [26] indicated that the Knight shift for V does not change markedly at T_c, which would render V unsuitable for the present study. However, as we have shown recently, in pure V the Knight shift definitely changes below T_c [27] as in pure Nb [28], which has a similar electronic structure.

In order to obtain a measurable spin polarization caused by the spin screening effect, the S-layer thickness in the S/F bilayer should be comparable with the SC coherence length in the S layer ξ_s because the perturbation of the spin susceptibility in the S layer is expected at a distance of the order ξ_s from the S/F interface only. Usually [25] for our V films $\xi_s \simeq 10$ nm, implying that the number of V nuclei involved in the resonance will be extremely small. In order to increase the number of

V nuclei subjected to the spin screening effect we used trilayer samples F/S/F (i.e., one S layer between two F layers) for our present investigation. This increases the perturbed by the spin screening effect S-layer thickness twice. On the other hand at the thickness of the S layer smaller than $3\xi_s$ superconductivity usually vanishes (see, e.g., [7, 25]). Therefore, the S-layer thickness in the F/S/F trilayer is limited to about $4\xi_s$. Even in this case conventional NMR spectrometers encounter serious sensitivity problems with this small sample volume and we had to develop a super sensitive NMR technique operating in a continuous mode to reach the necessary sensitivity.

2.2. *Experimental details. Samples.* We have prepared a number of F/S/F trilayers with V as the SC layer and either Ni or an alloy $Pd_{1-x}Fe_x$ as the ferromagnetic layers (see Table 1).

Table 1

Experimental parameters of all samples for the present study: S1 is the single V-layer, S2 is the $Pd_{0.98}Fe_{0.02}$/V/$Pd_{0.98}Fe_{0.02}$ trilayer, S3 is the $Pd_{0.97}Fe_{0.03}$/V/$Pd_{0.97}Fe_{0.03}$ trilayer, S4 and S5 are the Ni/V/Ni trilayers with thickness of the V-layer of 44 and 70 nm, respectively

	d_V (nm)	σ (nm)	T_c (K)	*RRR*	l (nm)	ξ_s (nm)
S1	30	0.3	4.7	11	15	14
S2	36	1.3	3.0	4.6	5	8
S3	42	1.3	3.6	6	7	10
S4	44	1.6	4.1	4.4	5	8
S5	70	0.8	4.4	8.2	11	12

The thickness and the quality of the films were characterized by small-angle x-ray reflectivity. Well resolved Kiessig fringes from the total layer thickness were clearly observed. Fits using the modified Parratt formalism [29, 30] yield the thickness of the V-layers d_V and the interface roughness parameter σ given in Table 1.

The SC transition temperature T_c for the samples in Table 1 is between 3 K and 4.7 K (see the fourth column of Table 1). From the ratio of the electrical resistivity at 300 K to its value at the temperature above T_c or the residual resistivity ratio $RRR = R(300\,\mathrm{K})/R(5\,\mathrm{K})$ (fifth column of Table 1) we can determine the specific residual resistivity ρ_0 using the phonon contribution to the specific resistivity for vanadium, $\rho_{\mathrm{phon}}(300\ \mathrm{K}) = 18.2$ $\mu\Omega\cdot$ cm. Following Lazar et al. [7] with the Pippard relations [31], we get $\rho_0 l = 2.5 \cdot 10^{-6}$ $\mu\Omega\cdot\mathrm{cm}^2$ and can calculate the mean free path l of the conduction electrons (6th column of Table 1). The BCS coherence length for V is $\xi_0 = 44$ nm. A comparison of l and ξ_0 implies that the superconducting parameters of our samples are closer to the "dirty" limit ($l \ll \xi_0$) than to the "clean" limit ($l \gg \xi_0$). In the "dirty" limit $\xi_s = \sqrt{\xi_0 l/3.4}$ holds, which is given in the last column of Table 1.

NMR spectrometer. We have built a continuous wave NMR spectrometer operating at the frequency of about 5.5 MHz [32] and based on a self-oscillating detector (see, e.g., [33]). Using the MESFET (metal semiconductor field effect transistor) CF739 capable of operating at temperatures below 4 K, we were able to immerse the high-frequency generator into the liquid helium in close vicinity to the pick-up coil. This strongly reduces the thermal noise and excludes losses in the line connecting the pick-up coil with the generator.

2.3 *Results and analysis. Normal state.* In Fig. 1a we show the NMR signals for the single V layer (sample

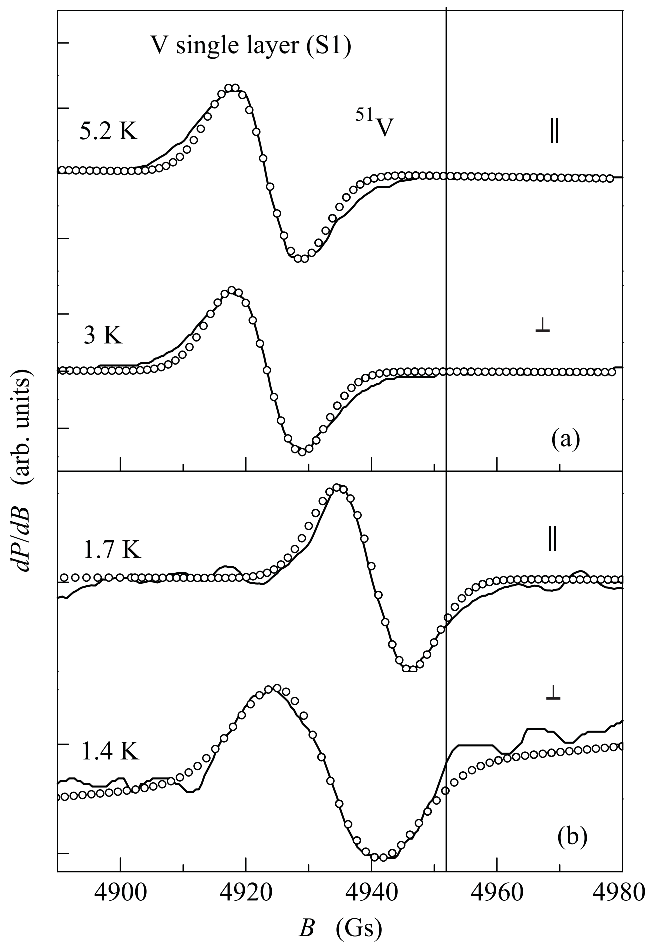

Fig. 1. NMR spectra for the single V layer (sample S1) in the normal (a) and superconducting (b) states for parallel (||) and perpendicular (⊥) orientation of dc magnetic field. The NMR spectra are fitted by the Gaussian line shape (circles). Here and in the following figures the vertical line shows the NMR line position for ^{51}V nuclei in an insulator

S1) in the normal state for the parallel and perpendicular orientation of the dc magnetic field relative to the film plane. The resonance line shape is well described by the derivative of a Gaussian absorption curve. Fitting this theoretical curve to the experimental spectra we can determine the resonance line position with an absolute accuracy better than 0.5 Gs. For the resonance linewidth (the peak-to-peak distance of the absorption line derivative) we get a value of ΔB =11.2 Gs. The resonance field of B_0^n=4923.1 Gs is shifted by δB = 29.1 Gs relative to its position in an insulator (4952.2 Gs for ^{51}V). Thus, for the Knight shift in the normal state, which is defined as the ratio of the NMR line shift relative to its position in an insulator, we get 0.59 ±0.01%, in good agreement with the value measured previously [26, 27]. The NMR line shape in the SC state is discussed in the next paragraph. Fig. 2a displays the NMR signals for a Ni/V/Ni trilayer (sample S4) in the normal state for both orientations of the magnetic field. For the field direction parallel to the film plane the resonance line position and the linewidth coincide nicely with that observed for the single V layer (Fig. 1a). For the perpendicular orientation of the field the NMR signal is shifted towards lower magnetic fields by 3 Gs and the line shape appears slightly distorted (the low field wing has a smaller amplitude than the high field wing). These observations are not surprising, since for the field directed parallel to the film plane the magnetization of the F layer lies in-plane and the demagnetizing field acting on the V layer is negligible. For the perpendicular orientation the demagnetizing field from the F layers is non-zero. We numerically estimated this dipolar field and obtained that this field slightly shifts the resonance line to the low field side and causes some line broadening with the degree of broadening comparable to the shift. As a result, the amplitude of the low field wing of the resonance line becomes slightly smaller than the amplitude of the high field wing, just as observed in the experiment. The calculated resonance line for the perpendicular direction is shown in Fig. 2a by crosses and it is obvious that there is satisfactory agreement with the experimental resonance lines.

Similar results were obtained in the normal state for $Pd_{1-x}Fe_x/V/Pd_{1-x}Fe_x$ trilayers with x= 0.02 (sample S2) and 0.03 (sample S3) for the field perpendicular to the film plane.

Superconducting state. In Fig. 1b the NMR spectrum for the single V layer (sample S1) below T_c for both field orientations is depicted. Compared to the normal state (Fig. 1a) the resonance line is shifted towards higher magnetic fields and definitely broadened in case of the perpendicular orientation (ΔB=15.5 Gs).

Vanadium is a type II superconductor and for the perpendicular orientation the V film is in the vortex

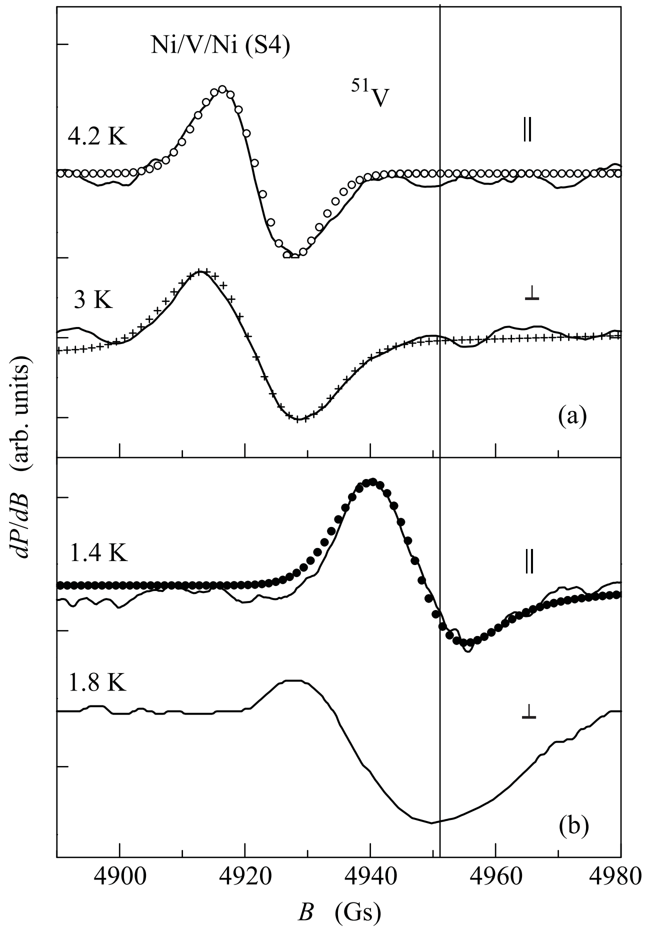

Fig. 2. NMR spectra for Ni/V/Ni trilayer (sample S4) in the normal (a) and superconducting (b) states for the parallel(||) and perpendicular (⊥) orientations of the filed. The NMR spectrum for the normal state in the parallel orientation is fitted by the Gaussian line shape (open circles), and in the perpendicular orientation by the Gaussian line shape taking the demagnetizing field from the F layers into account (crosses). The fit for the superconducting state in parallel orientation takes the spin screening effect with B_m=15 Gs (see Eqs. 1 and 2) into account (closed circles)

state. The broadening and shift of the NMR line upon the transition to the SC state is caused by the inhomogeneous magnetic field distribution in the vortex state. The NMR line shape in the mixed state of type II superconductors is determined by the convolution of the normal state line shape and the singular distribution of the magnetic field in the vortex state (see, e.g., [28, 34, 35]). For our samples with $\kappa \simeq 3 \div 4$ the pinning forces lead to a transformation of the singular field distribution to a Gaussian shape [36] with a width estimated as $\delta B_v \sim (B_{c2} - B_0)/2\kappa^2$. With $B_{c2} \simeq$5000 Gs and B_0=4920 Gs this gives $\delta B_v \sim$ 3.5 Gs. If the NMR line shape in the normal state is Gaussian, then in the SC state it should keep its Gaussian shape with some additional broadening δB_v as estimated above. This is just what we have observed in our experimental spectrum for the single vanadium film (sample S1). (See evolution of the NMR linewidth from Fig. 1a (normal state, ΔB=11.2 Gs) to Fig. 1b (SC state with ΔB=15.5 Gs)). Upon the transition to the SC state the line shape does not change markedly, the resonance field increases up to B_0^s=4943 Gs, and an additional Gaussian broadening $\delta B_v^{\rm exp} \simeq$4.3 Gs is observed. The vortexes motion and their depinning leads to the appearance of the regular noise in Fig. 1b.

For the single V film (Fig. 1b) in the parallel orientation, we first note that, similar to the perpendicular orientation, the NMR line shifts to higher fields compared to the normal state. However, in contrast to the perpendicular orientation, the NMR linewidth does not markedly differ from the normal state. This supports our assumption above that the broadening in the perpendicular orientation is caused by the presence of vortices. In its turn we assume that for the parallel orientation of vortices are absent. Following to the analysis by Burger et al. [37] we conclude that at the field parallel to the plane of films our samples are in vortex-free state. Thus, the magnetic field inside the V layer decays exponentially from both surfaces with the decay length given by the magnetic penetration depth λ. Numerical calculations show that in our case for d_V ~30 nm and λ ~50 nm the inhomogeneity of the magnetic field distribution virtually does not influence the NMR line width, because the magnetic field is strongly inhomogeneous only in the close vicinity of the film surface. Convolution of the field distribution with a Gaussian line shape in this case leads to the shift of the resonance line by less than 1 Gs and to a small distortion of the resonance line wings only.

Figure 2b shows the NMR spectra for Ni/V/Ni trilayer (sample S4) in the SC state for both orientations of magnetic field. Similar to the case of the single V layer we observe a shift of the resonance line to higher magnetic fields. At the same time, however, the line shape for both field directions is markedly changed with the high-field wing of the NMR line strongly distorted.

The same anomalous change of the NMR line shape we also observe for the NMR spectra in $\mathrm{Pd}_{1-x}\mathrm{Fe}_x/\mathrm{V}/\mathrm{Pd}_{1-x}\mathrm{Fe}_x$ trilayers with x= 0.02 (sample S2) and 0.03 (sample S3) in the SC state.

We also studied the evolution of the NMR line shape with increasing S-layer thickness for Ni/V/Ni trilayer samples (Fig. 3). One sees that the distortion of the high-field wing of the resonance line has an obvious trend to disappear with increasing V-layer thickness.

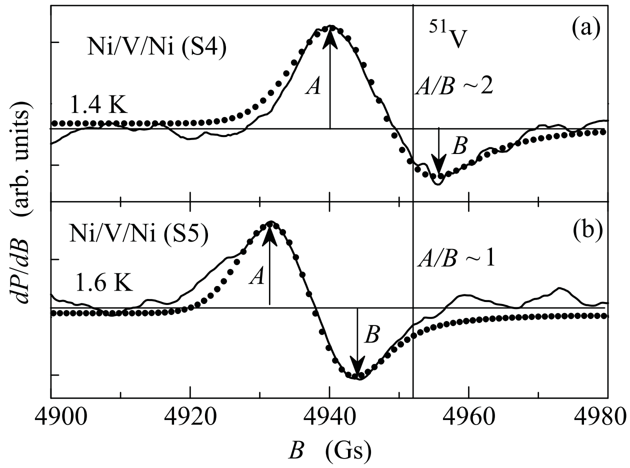

Fig. 3. NMR spectra for Ni/V/Ni trilayers (samples S4 with d_V=44 nm and S5 with d_V=70 nm) in the superconducting state (parallel magnetic field). The theoretical fits take the spin screening effect with B_m=15 Gs (see Eqs. 1 and 2) into account (closed circles)

2.4. *Discussion*. The central result of this study is that the NMR line shape of the F/S/F trilayers definitely changes on the transition to the SC state. The line shape for the sample S4 in the SC state is reminiscent of the classical calculation by Bloembergen [38] for the NMR line shape in the metallic samples with a thickness d comparable to the electrodynamic skin-depth δ. The line shape asymmetry parameter A/B (the ratio of low-field peak height A to the high-field peak height B) varies from 1.0 for fully transparent films ($d \ll \delta$) to 2.55 for a half-space ($d \gg \delta$). This distortion results from electrodynamic admixture of the dispersion component of the dynamic magnetic susceptibility to the absorption component. For a metallic half-space, the detected NMR signal is a one-to-one mixture of the absorption and dispersion, and the asymmetry parameter reaches its maximum magnitude A/B=2.55. At our NMR frequency 5.5 MHz, the skin depth is about 50 μm. Thus in the normal state samples with a total thickness of the order of 40÷70 nm are completely transparent for the radio frequency radiation, hence, no electrodynamic distortion of the NMR line shape is expected.

Analysis shows that other possible origins of a distorted NMR line like an inhomogeneous distribution of the quadrupole splitting at the MgO/V or the Ni/V interfaces due to the lattice mismatch and the local field distribution in the vortex state can also be ruled out.

One important experimental feature of the distortion is that it disappears with increasing V thickness, clearly indicating that there is a mechanism determining the line shape below T_c only acting in the vicinity of the interfaces at a distance of the order of ten to twenty nanometers. When the SC Vanadium layer is thick, the NMR signal from the unperturbed core of the film dominates in the NMR response, and the symmetry of the line shape is being restored: the asymmetry parameter A/B approaches 1. Recollecting all findings concerning the NMR line distortion we are led to the conclusion that the spin screening effect as discussed in the Introduction is the most plausible mechanism giving rise to the NMR line distortion observed experimentally.

According to the model of the spin screening effect [8], spin-polarized electrons from the interfacial region penetrate into the SC layer. By means of the hyperfine interaction this spin-polarization induces a local field $B_{\rm loc}$ on the V nuclei with a direction opposite to the external magnetic field (we suppose that the conduction electron spin polarization in the F layer is in the direction of the applied field) and the NMR resonance field shifts to higher fields accordingly.

In order to calculate the NMR line shape quantitatively, one must take the spatial distribution of the spin polarization in the SC layer into account. The induced spin-polarization in the superconductor which is proportional to the local magnetic field $B_{\rm loc}$ decays exponentially with the distance x from both F/S interfaces,

$$P(x) \sim B_{\rm loc} = B_m \cosh(k_s x), \tag{1}$$

where the x-axis is perpendicular to the S/F interface and x=0 corresponds to the center of the SC layer, $k_s = 1/\xi_s$ and B_m is the value of the local field at the S/F interfaces. The local field distribution,

$$F(B) = \frac{1}{d}\int_0^d dx\delta[B - B_{\rm loc}(x)] \tag{2}$$

has to be convoluted with the unperturbed NMR Gaussian line shape derived from the normal-state NMR line above T_c.

Fitting the NMR line shape with the local field modified by the spin screening effect is straightforward for the case of the parallel field direction, since in this case the film is in the vortex-free state and there are no complications due to the inhomogeneous local field distribution in the vortex state. As seen in Fig. 1b, the NMR line for the single V layer in the parallel orientation of the sample simply shifts to higher fields without any broadening below T_c.

The fits taking the spin screening effect into account (Figs. 2b and 3) show a reasonable agreement with the experimental line shape. We obtain a parameter $B_m \simeq$15 Gs which represents the maximum shift of the resonance line for nuclei in close vicinity of the S/F interface. The resonance field value was taken as a free parameter in the fit.

We next want to try a quantitative comparison of B_m resulting from the fit and the corresponding theoretical model of the spin screening effect by Bergeret et al. [8]. Within this model the local magnetic field producing the polarization of conduction electrons at the interface is given by

$$B(\pm d_s/2) = \alpha 4\pi M_F(d_f/\xi_s). \tag{3}$$

Here α denotes the part of the magnetization of the ferromagnet caused by the conduction electrons. Using the saturation magnetization of Ni M_F=515 Gs and supposing that metallic Ni is an ideal itinerant ferromagnet ($\alpha \simeq$1) we get $B(d_s/2) \simeq$3 kG. This field produces the polarization of the conduction electrons in the SC layer and via the contact interaction shifts the NMR line.

Fig. 1 shows that in the parallel orientation of the single V film the NMR resonance field in the normal state is B_0^n =4923.1 Gs. The shift of the resonance line relative to the position in an insulator (4952.2 Gs) is δB=29.1 Gs. In the SC state the resonance field is B_0^s = 4943 Gs (Fig. 1). As mentioned above, our estimation shows that the diamagnetism of the film due to the Meissner effect contributes less than 1 Gs to the shift of the resonance field. Therefore the shift of the NMR line by $B_0^s - B_0^n \simeq$20 Gs at the transition into the SC state is solely due to the change of the Knight shift i.e. the change of the electron polarization at the V core produced by an external magnetic field of about 5 kG. This provides a suitable reference for the calculation of the parameter B_m=15 Gs, the spin screening parameter which we have fitted above in Figs. 2b and 3. In the theory of the spin screening effect B_m is caused by the induction of Ni at the interfaces $B(\pm d_s/2) \simeq$3 kG. With the relation between the induction and change of the Knight shift in the SC state (5 kG gives a shift $\delta B \simeq$20 Gs) the theory predicts $B_m \simeq$12 Gs, in good agreement with B_m=15 Gs derived experimentally.

For the perpendicular orientation of the magnetic field, one must take into account the local field distribution due to the spin screening effect as well as the inhomogeneous field distribution due to the vortex state. We didn't try to fit these spectra quantitatively and just present qualitatively the tendency of the broadening of the high-field wing of the NMR line for the S2, S3 and S4 trilayer samples.

3. Spin valve effect. 3.1 *Superconducting spin valves based on epitaxial* Fe/V *superlattices.*

As it follows from the Introduction recently [19] a SC V film grown on an epitaxial [Fe/V] superlattice with antiferromagnetic interlayer exchange coupling demonstrated that its SC transition temperature T_c depends on the relative orientation of the magnetization direction of subsequent Fe layers in the [Fe/V]-superlattice. We observed a shift ΔT_c=120 mK for a 18 nm thick V-film on a [Fe(2 ML)/V(12 ML)]$_{25}$-superlattice (here ML is monolayer and 25 is the number of repetitions) [19]. This is nearly one order of magnitude larger than observed for the F1/S/F2-type spin valves up to now. In continuation of our previous work [19] we first studied F1/N/F2/S-type structures and investigated the spin valve effect for F1 and F2 layers with different composition, thickness and quality [39]. In Fig. 4 we have plotted

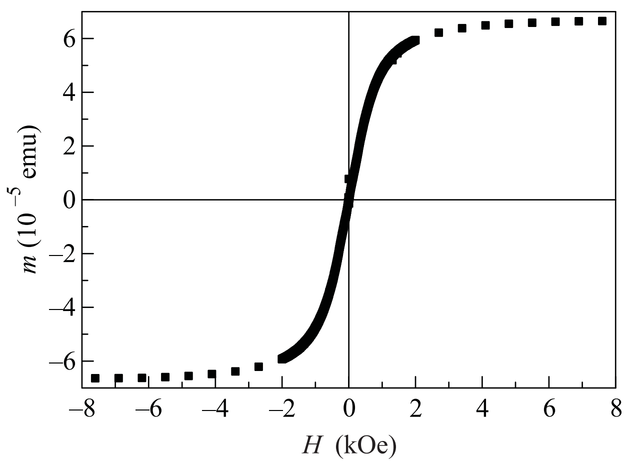

Fig. 4. Magnetic moment versus magnetic field (direction in the film plane) measured at 10 K for the sample V(24nm)/[Fe(3ML)/V(12ML)]$_{25}$

a magnetization curve measured at 10 K for the sample V(24nm)/[Fe(3ML)/V(12ML)]$_{25}$. The magnetization curve reveals antiferromagnetic interlayer exchange coupling of the Fe layers in the superlattice. The ferromagnetic saturation field of the Fe sublattice is about 2.2 kOe. In this sample the magnetization direction of subsequent Fe layers in the superlattice can be gradually rotated from an antiparallel alignment in zero field to a parallel alignment for fields above 2 kOe. The square of the upper critical magnetic field for the direction parallel to the film plane $(H_{c2}^P(T))^2$ is plotted in Fig. 5. For a two dimensional (2D) thin film with the magnetic field parallel to the film plane the classical result for the upper critical field is [40]:

$$H_{c2}^P(T) = \frac{\Phi_0}{2\pi\xi^2(0)} \frac{\sqrt{12}}{d_s} \sqrt{\left(1 - \frac{T}{T_c}\right)} \qquad (4)$$

with the flux quantum Φ_0, the thickness of the film d_s and the Ginzburg-Landau correlation length ξ, which is related to Pippard's correlation length by $\xi(0) = 1.6\xi_s$. We have performed measurements of the upper critical

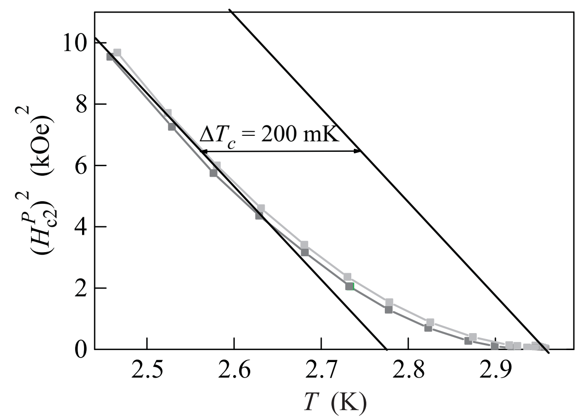

Fig. 5. Squared parallel upper critical magnetic field versus temperature for the same sample as in Fig. 4. The solid straight line (left line) describes the temperature dependence for $(H_{c2}^P)^2$ above 5 kOe^2. This line indicates the upper critical fields expected for perfect parallel alignment of the Fe layers in the superlattice. Another straight line shows the $(H_{c2}^P)^2$ vs temperature for unchanged mutual orientation of magnetizations of the subsequent Fe layers in multilayer

field for Fe/V/Fe trilayers and obtained that for parallel orientation of the magnetic field relative to the film plane $H_{c2}(T)$ is perfectly described by formula (4).

In Fig. 5 we have plotted the straight line which describes the temperature dependence for fields above 2 kOe perfectly. Below the ferromagnetic saturation field of the superlattice at about 2 kOe there is an increasing deviation from the straight line. From the extrapolation of the straight line one gets a SC transition temperature T_c which is more than 200 mK below the true transition temperature measured at zero field. A comparison with the magnetization curve of the V(24nm/[Fe(3ML)/V(12ML)]$_{25}$-superlattice in Fig. 4 shows that the ferromagnetic saturation field of 2 kOe is correlated with the first deviation of H_{c2}^P from the straight line in Fig. 5. From this we infer that the deviation of the upper critical field from the 2D-behavior is caused by the gradual change of the sublattice magnetization direction of the [Fe(3ML)/ V(12ML)]$_{25}$ superlattice from parallel above 2 kOe to antiparallel in zero field. The obtained difference in T_c of 200 mK for the superlattice being in the antiparallel and the parallel orientation. This corresponds to the SC spin valve effect observed in [Fe(2ML)/V(11ML)]$_{25}$/V-systems before [19]. However, the maximum shift ΔT_c we have observed in [19] was only about 120 mK, definitely smaller than for the present sample. We think that this reflects the improved quality of our new samples with ξ_s/d_s=0.67 for the sample in Fig. 5 compared to a maximum value of ξ_s/d_s=0.4 for the samples in [19].

3.2. *Full spin switch effect for the superconducting current in an* S/F *thin film heterostructure.* Comparison of the results obtained for both proposed constructions of the spin switches F1/F2/S and F1/S/F2 (see the Introduction) gives grounds to suppose that the scheme by Oh et al. [12] may be more promising for the realization of the full spin switch effect. We have fabricated a set of samples MgO(001)/CoO_x/Fe1/Cu/Fe2/In which show a full switching between the SC and normal states when changing the mutual orientation of the magnetizations of F1 and F2 layers [41]. In this construction MgO(001) is a high quality single crystalline substrate, cobalt oxide antiferromagnetic (AFM) layer plays a role of the bias layer which pins the magnetization of the F1 layer; Fe stands for the ferromagnetic F1 and F2 layers; Cu as a normal metallic N layer which decouples the magnetizations of F1 and F2 layers; finally In is an S layer.

The residual resistivity ratio $RRR=R(300\text{K})/R(4\text{K})$ is similarly high for all studied samples (see Table 2) evidencing a high purity of the deposited In layers.

Using the ferromagnetic resonance measurements we adjusted the long axis of our films to be along the easy axis of the magnetization which is induced by residual magnetic fields in our vacuum system. The parameters of the studied samples are shown in Table 2. Along with the spin switch samples ## 3 – 5 we prepared for control purposes an indium thin film sample (#1) and a reference sample comprising an indium layer and only one F layer (#2R). In a first step the in-plane magnetic

Table 2

Experimental parameters of the studied samples

	Thickness (nm)			δT_c	ΔT_c
	Fe2	In	RRR	(mK)	(mK)
1		220	43	7	0±2
2R	0.5	230	35	15	0±3
3	0.5	230	47	7	19±2
4	0.6	230	41	13	12±2
5	2.6	230	44	50	-2±8

hysteresis loops of sample #3 in the direction of the magnetic field along the easy axis was measured by a SQUID magnetometer and is shown in Fig. 6. This step is necessary to obtain the Fe-layers' magnetization behavior and to determine the magnetic field range where AP and P states can be achieved. The sample was cooled down in a magnetic field of +4 kOe applied parallel to the sample plane and measured at $T = 4$ K. The magnetic field

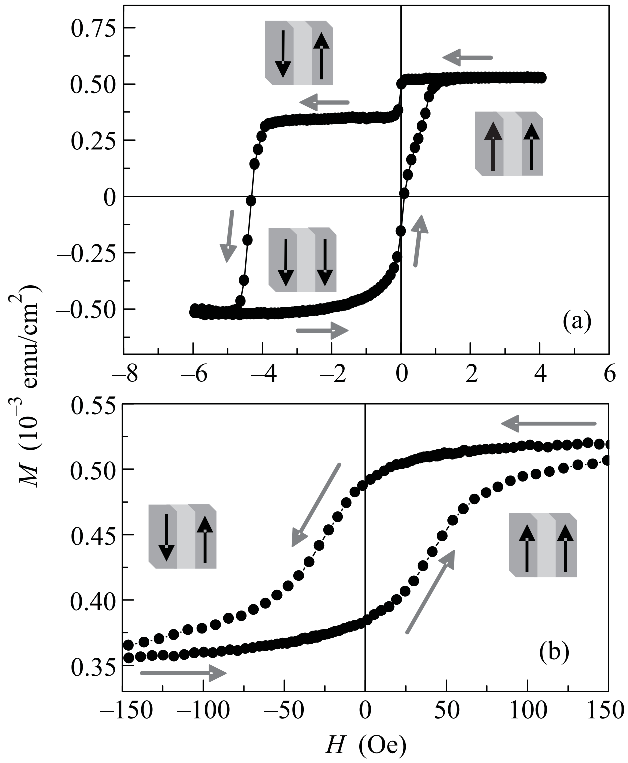

Fig. 6. (a): Magnetic hysteresis loop for sample #3. Panel (b) shows part of the minor hysteresis loop for sample #3, obtained when decreasing the magnetic field from +4 kOe down to −1 kOe and increasing it up to +1 kOe. The amplitude of the minor hysteresis loops is proportional to the thickness of the free F2 layer. Coercive and saturation fields are the largest for the sample #3 and sharply decrease with increasing d_{Fe2}

was varied from +4 kOe to – 6 kOe and back again to the value of +4 kOe. Both limits correspond to the orientation of the magnetizations of the F1 and F2 layers parallel to the applied field. For the studied sample by decreasing the field from +4 kOe to the field value of the order of +50 Oe the magnetization of the free F2 layer starts to decrease. At the same time the magnetization of the F1 layer is kept by the bias CoO_x layer until the magnetic field of −4 kOe is reached. Thus, in the field range between −0.3 and −3.5 kOe the mutual orientation of two F layers is antiparallel. Below $H = -3.5$ kOe the magnetization of the F1 layer starts to change it's value and at the field of the order of −4.5 kOe magnetizations of both Fe layers become parallel. This corresponds to a further step-like decrease of the total magnetization. Qualitatively similar hysteresis loops were obtained for samples #4 and 5. The minor hysteresis loops on the low field scale were obtained with decreasing the field from +4 kOe down to −1 kOe and increasing it again up to +1 kOe. An exemplary loop for sample #3 is shown in Fig. 6b.

In order to study the influence of the mutual orientation of the magnetizations on T_c we have cooled the samples down from room to a low temperature at the magnetic field of 4 kOe applied along the easy axis of the sample just as we did it when performing the SQUID magnetization measurements. For this field both F-layers' magnetizations are aligned (see the magnetic hysteresis loops shown in Fig. 6). Then at the in-plane magnetic field value of $H_0 = \pm\ 110$ Oe the temperature dependence of the resistivity R was recorded. In the following we focus on the spin valve sample # 3 (see Fig. 7). For this sample $\Delta T_c = T_c^{AP} - T_c^{P}$ =19 mK (see Fig. 7b with an enlarged temperature scale). We also performed similar resistivity measurements of the reference sample #2R with only one Fe layer (see Table 2). For this sample we found T_c=1.60 K, which does not depend on the magnetic field direction (see Fig. 7c). This T_c value is lower than that for the In single layer film (sample #1) and higher than for sample #3 (Fig. 7a). This means that T_c is suppressed by the F2 layer and in turn is sensitive to the influence of the F1 layer separated from the SC In layer by a 0.5 nm thick F2 Fe layer and 4 nm thick Cu layer. As can be expected from the the S/F proximity theory, with increasing the thickness of the free F2 layer ΔT_c decreases and becomes practically zero at 2.6 nm thick F2 layer (see Table 2).

The observed shift ΔT_c=19 mK is not the largest one among the data published before (cf., e.g., Ref. [17], where $\Delta T_c \simeq 41$ mK at $\delta T_c \sim$100 mK). However, very importantly it is substantially larger than δT_c which is of the order of 7 mK for sample #3 at H_0=110 Oe. This opens a possibility to switch off and on the SC current flowing through our samples *completely* within the temperature range corresponding to the T_c-shift by changing the mutual orientation of magnetization of F1 and F2 layers. To demonstrate this we have performed the measurements of the resistivity of sample #3 by sweeping slowly the temperature within the ΔT_c and switching the magnetic field between +110 and −110 Oe. This central result of our study is shown in Fig. 7b. It gives straightforward evidence for a complete on/off switching of the SC current flowing through the sample. For sample #3 the main necessary prerequisite to realize the theoretical idea of Oh et al. [12] is fulfilled. In this sample d_{Fe2} is smaller than ξ_F. Finally, the high quality of the iron layers yields magnetization hysteresis curves with sharp well defined steps enabling a well controlled switching of the mutual orientation of the magnetization of the F layers by application of relatively small magnetic fields.

4. Summary and conclusions. We find first qualitative and quantitative manifestations of the spin screening effect in the SC state, as evidenced by a characteristic

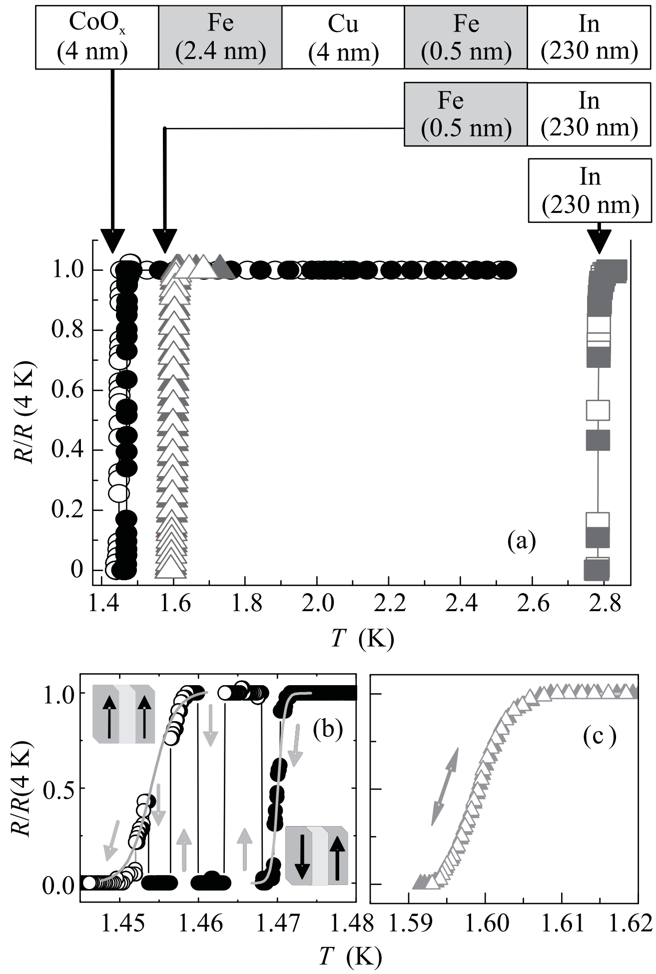

Fig. 7. (a): Overview of the resistivity transition curves. The spin valve sample #3 is shown by open ($H_0 = +110$ Oe) and closed ($H_0 = -110$ Oe) circles (for details see (b)). For the reference sample #2R the data are depicted by open ($H_0 = +110$ Oe) and closed ($H_0 = -110$ Oe) triangles (for details see (c)). For the pure In sample the data are presented by open ($H_0 = +110$ Oe) and closed ($H_0 = -110$ Oe) squares. (b): Switching between normal and SC states in the spin valve sample #3 during a slow temperature sweep by applying the magnetic field $H_0 = -110$ Oe (closed circles) and $H_0 = +110$ Oe (opened circles) in the sample plane

asymmetry of the NMR line shape below T_c in the S/F layered thin film system. Simultaneously another possibility to detect the spin screening effect was demonstrated by Xia et al. [42] who used the optical polar Kerr effect on Al/Co-Pd bilayers and observed a small change of the Kerr rotation below T_c of Al.

An anomalous shift $\Delta T_c \simeq$200 mK was observed for V layer deposited on [Fe/V] superlattice when rotating the mutual orientation between magnetizations of two successive Fe layers of superlattice. However, in this system the relative orientation of magnetizations can be changed only gradually from antiparallel to parallel with increasing the magnetic field value from 0 to 6 kOe.

And, finally, using the spin switch design F1/F2/S theoretically proposed by Oh et al. [12], that comprises a ferromagnetic bilayer as an F component, and an ordinary superconductor as the second interface component, we have realized a full spin switch effect for the SC current. An experimental realization of this spin switch construction was achieved for the CoO_x/Fe1/Cu/Fe2/In multilayer.

This review is based on the results obtained within the project No. 08-02-00098 of the Russian Foundation for Basic Research (RFBR). Now the continuation of this work is supported by the RFBR (Grant No. 11-02-01063).

---

1. I. A. Garifullin, J. M. M. M. **240**, 571 (2002).
2. Yu. A. Izyumov, Yu. N. Proshin, and M. Khusainov, Uspehi Fizicheskih Nauk **172**, 113 (2002) [Phys. - Uspekhi. **45**, 109 (2002)].
3. A-I. Buzdin, Rev. Mod. Phys. **77**, 945 (2005).
4. F. S. Bergeret, A. F. Volkov, and K. B. Efetov, Rev. Mod. Phys. **77**, 1321 (2005).
5. K. B. Efetov, I. A. Garifullin, A. F. Volkov, and K. Westerholt, *Magnetic Heterostructures. Advances and Perspectives in Spinstructures and Spintransport*. Series Springer Tracts in Modern Physics, Vol. **227**. Zabel H., Bader S. D. (Eds.), 2007, p. 252.
6. Z. Radović , L Dobrosavljevic-Grujić, A. I. Buzdin, and John A. Klem, Phys. Rev. B **38**, 2388 (1988).
7. L. Lazar, K. Westerholt, H. Zabel et al., Phys. Rev. B **61**, 3711 (2000).
8. F. S. Bergeret, A. F. Volkov, and K. B. Efetov, Europhys. Lett. **66**, 111 (2004); Phys. Rev. B **69**, 174504 (2004).
9. M. Yu. Kharitonov, A. F. Volkov, and K. B. Efetov, Phys. Rev. B **73**, 054511 (2006).
10. G. Deutscher and F. Meunier. Phys. Rev. Lett. **22**, 395 (1969).
11. T. W. Clinton and M. Johnson. Appl. Phys. Lett. **70**, 1170 (1997).
12. S. Oh, D. Youm, and M. R. Beasley. Appl. Phys. Lett. **71**, 2376 (1997).
13. L. R. Tagirov. Phys. Rev. Lett. **83**, 2058 (1999).
14. A. I. Buzdin, A. V. Vedyaev. and N. N. Ryzhanova. Europhys. Lett. **48**, 686 (1999).
15. J. Y. Gu, C. Y. You, J. S. Jiang et al., Phys. Rev. Lett. **89**, 267001 (2002).
16. A. Potenza and C. H. Marrows, Phys. Rev. B **71**, 180503(R) (2005).
17. I. C. Moraru , Jr. W. P. Pratt, and N. O. Birge, Phys. Rev. Lett. **96**, 037004 (2006).
18. Guo-Xing Miao, Ana V. Ramos, and J. Moodera, Phys. Rev. Lett. **101**, 137001 (2008).
19. K. Westerholt, D. Sprungmann, H. Zabel et al., Phys. Rev. Lett. **95**, 097003 (2005).
20. R. I. Salikhov, I. A. Garifullin, N. N. Garif'yanov et al., Phys. Rev. Lett. **102**, 087003 (2009).
21. R. I. Salikhov, N. N. Garif'yanov, I. A. Garifullin, Phys. Rev. B **80**, 214523 (2009).
22. J. R. Schrieffer, *Theory of superconductivity*, New York: W. A. Benjamin, 1964.
23. D. E. MacLaughlin, *Solid State Physics*, Eds. F. Seitz and D. Turnbull, Academic Press, Inc., New York, 1976, Vol. **31**, p. 1.
24. P. Isberg, B. Hjrvarsson, R. Wräppling et al., Vacuum **48**, 483 (1997).
25. I. A. Garifullin, D. A. Tikhonov, N. N. Garif'yanov et al., Phys. Rev. B **66**, 020505(R) (2002).
26. B. J. Noer and W. D. Knight, Rev. Mod. Phys. **36**, 177 (1964).
27. I. A. Garifullin, N. N. Garif'yanov, R. I. Salikhov, and L. R. Tagirov, Pis'ma v Zh. Eksp. Teor. Fiz. **87**, 367 (2008) [JETP Lett. **87**, 317 (2008)].
28. D. Rossier and D. E. MacLaughlin, Phys. Kondens. Materie **11**, 66 (1970).
29. L. C. Parratt, Phys. Rev. **95**, 359 (1954).
30. L. Nevot and Crose, Rev. Phys. Appl. **15**, 761 (1980).
31. A. B. Pippard, Rep. Progr. Phys. **23**, 176 (1960).
32. In order to observe the NMR in the SC state the resonance field should be smaller than the critical field of superconductor. For the chosen frequency the NMR of ^{51}V nuclei occurs at the magnetic field of the order of 5 kOe (see Figs. 1–3).
33. K. J. Wilson and C. P. G. Valabhan, Meas. Sci. Technol. **1**, 458 (1990).
34. J.-M. Delriew, Solid State Commun. **8**, 61 (1970).
35. L. Dobrosavljevic, C. R. Acad. Sci. Paris **263**, 502 (1966).
36. E. H. Brandt, J. Low Temp. Phys. **73**, 355 (1988).
37. J. P. Burger, G. Deutscher, E. Guyon, and A. Martinet, Phys. Rev. **137**, A853 (1965).
38. N. Bloembergen, J. Appl. Phys. **23**, 1383 (1952).
39. G. Nowak, H. Zabel, K. Westerholt et al., Phys. Rev. B **78**, 134520 (2008).
40. P. G. de Gennes and M. Tinkham, Physics **1**, 107 (1964).
41. P. V. Leksin, N. N. Garif'yanov, I. A. Garifullin et al., Appl. Phys. Lett. **97**, 10505 (2010).
42. J. Xia, V. Shelukhin, M. Karpovski et al., Phys. Rev. Lett. **102**, 087004 (2009).